scientific reports

OPEN

Combined impact of semantic segmentation and quantitative structure modelling of Southern pine trees using terrestrial laser scanning

Jinyi Xia[1]✉, Timothy A. Martin[1], Gary F. Peter[1], Kody M. Brock[1], Jeff W. Atkins[2], Matthew A. Gitzendanner[3], Inacio Bueno[1], Kim Calders[4], Ana Paula Dalla Corte[5], Andrew T. Hudak[6], Monique Bohora Schlickmann[1], Michael G. Andreu[1], Caio Hamamura[7], Carine Klauberg[1] & Carlos A. Silva[1]✉

Southern pine forests play a key role in the ecological function and economic vitality of the southeastern United States. High-resolution terrestrial laser scanning (TLS) has become an indispensable tool for advancing tree structural research and monitoring. A critical challenge in this field is the accurate segmentation of leaf and wood components, which directly impacts the reliability of Quantitative Structure Models (QSMs). Segmentation techniques have progressed, but most existing methods are tailored for broadleaf species, with limited exploration for coniferous species such as southern pines. Addressing this gap, our study evaluates the performance of multiple segmentation algorithms on TLS data from southern pines, providing valuable insights into improving structural analysis and supporting more precise and efficient forest research and monitoring methodologies. We collected TLS data from longleaf pine (*Pinus palustris* Mill.) and loblolly pine (*Pinus taeda* L.) trees in Florida, USA, and compared the performance of four segmentation algorithms: TLSep, Graph, DBSCAN, and KPConv to separate leaf and wood. We found that KPConv was the most accurate method of segmenting wood and leaf points, with an overall accuracy (OA) of 98% and F1 score of 98% for loblolly pine and 95% and 94%, respectively, for longleaf pine. Although KPConv requires a substantial initial investment for training, its inference time is fast, making it a strong candidate for high-accuracy large-scale applications. These results led to highly reliable QSMs across trunk, branch, and total volume estimates. In contrast, DBSCAN, while slightly less accurate (OA of 92% for loblolly pine and 90% for longleaf pine), does not require training data and offers a favorable trade-off between performance and efficiency. These findings highlight the importance of selecting segmentation algorithms based on specific research goals, balancing accuracy and computational feasibility in forest structural modeling.

Keywords 3D point cloud, Wood point segmentation, Artificial intelligence, LiDAR

Southern pine forests are crucial to both the ecological function and economic vitality of the southeastern United States[1]. They contribute 63% of the United States' softwood timber removals[2] and recent studies project that this region will continue to lead timber production for the next 50 years[3]. Beyond their economic significance, southern pine forests offer essential ecosystem services such as soil conservation, habitat provision, water regulation, and carbon sequestration, which are key to environmental sustainability[4]. These forests primarily

[1]School of Forest, Fisheries, and Geomatics Sciences, University of Florida, Gainesville, FL 32611, USA. [2]USDA Forest Service Southern Research Station, New Ellenton, SC 29809, USA. [3]Department of Biology, University of Florida, Gainesville, FL 32611, USA. [4]Q-ForestLab – Laboratory of Quantitative Forest Ecosystem Science, Department of Environment, Ghent University, Ghent 9000, Belgium. [5]Department of Forest Engineering, Federal University of Paraná (UFPR), Curitiba, PR, Brazil. [6]USDA Forest Service Rocky Mountain Research Station, Moscow, ID 83843, USA. [7]Federal Institute of Education, Science and Technology of São Paulo, São Paulo 11533-160, Brazil. ✉email: jinyixia@ufl.edu; c.silva@ufl.edu

consist of loblolly pine (*Pinus taeda* L.), shortleaf pine (*Pinus echinata* Mill.), longleaf pine (*Pinus palustris* Mill.), and slash pine (*Pinus elliottii* Engelm.)[5]. Among these species, longleaf and loblolly pines are particularly notable for their substantial ecological and economic contributions. Longleaf pine forests are ecosystems rich in biodiversity, offering essential habitats for numerous endangered species[6]. In contrast to longleaf pine dominated forests, loblolly pines are valued for their rapid growth rates and are widely used in commercial pine plantations, highlighting their importance in the timber market[2].

A detailed understanding of stem and branch structure is crucial to many forest science and monitoring applications, as these traits directly influence wind resistance, growth dynamics, and carbon storage capacity[7]. However, traditional forest ground-based surveys and sample plot inventory methods are time-consuming, labor-intensive, and susceptible to human error[8]. Since the early 2000 s, terrestrial laser scanning (TLS) has been adopted as a powerful tool for forest monitoring and vegetation mapping[9]. TLS emits laser pulses to measure distances from the scanner to surrounding objects, producing high-density point clouds that allow for rapid, accurate 3D modeling of forest plots and precise estimation of tree structural attributes[8,10]. More recently, TLS has been applied to reconstruct quantitative structure models (QSMs), which provide a non-destructive means to estimate volume and allometric traits of aboveground biomass (AGB) components[11]. QSMs offer detailed insights into tree architecture, enabling precise measurements of tree volume. These models have been widely validated across various forest types[12–15] demonstrating their effectiveness for structural analysis and accurate volume estimation.

A critical step in constructing reliable QSMs with TLS data is the accurate segmentation of leaf and wood points (i.e., semantic segmentation), as misclassification can result in the model producing unrealistically thick or nonexistent branches, which overestimate both volume and AGB[12]. Proper separation of these points is necessary to capture the exact size, shape, and arrangement of branches within the point cloud[16] which is fundamental to producing high-quality QSMs from TLS data[17]. For instance, TreeQSM, one of the most widely used QSM applications, only accepts input based on returns from the wood component[18]. Methods for separating wood and leaf sections fall into three categories: radiometric-based, geometric-based, or a combination of both[17,19]. Radiometric approaches rely on the differing reflectance properties of wood and leaves, making intensity calibration a key step[20,21]; however, determining the precise threshold for accurate separation remains challenging[22]. On the other hand, geometric-based methods, which depend solely on the three-dimensional coordinates of the points[23] are more commonly employed due to their adaptability across data from various sensors[24].

Although the separation of leaf and wood components in TLS data has been extensively studied, most existing research focuses on datasets obtained from broadleaf species[17,19,24]. However, methods developed for broadleaf trees often do not generalize well to conifers due to key structural differences[25]. Broadleaf species typically have large, flat leaves and distinct branching, whereas conifers have exhibit needle-like foliage and densely packed, overlapping crowns. These characteristics reduce the spatial separation between leaf and wood points in the point cloud, making classification more difficult[26]. Due to these differences, segmentation methods originally developed for broadleaf species have not been extensively evaluated on coniferous trees. While some studies address leaf and wood point separation in coniferous trees[27–32] the number and scope of these studies are limited, and they often do not fully consider the unique structural characteristics of these species. Moreover, while several studies have proposed novel algorithms for leaf and wood separation in conifers, the majority have concentrated on improving classification accuracy without thoroughly examining the subsequent effects on QSM construction. Specifically, there is a noticeable lack of systematic comparisons that assess how different leaf and wood separation methods impact the accuracy of QSM-derived volume estimates. Additionally, some of the algorithms employed in these studies are proprietary, limiting their accessibility and practical application.

This study aims to fill these gaps by assessing several open-source QSMs and leaf and wood segmentation algorithms to identify the most effective pipeline for accurately predicting branch and stem volumes in southern pine trees. The specific objectives were to: (i) evaluate the accuracy of four geometric-based leaf and wood segmentation approaches in southern pine trees; (ii) select the most robust and accurate QSM model for our dataset; and (iii) assess the effect of leaf and wood segmentation accuracy on phenotypic characteristics generated by QSMs. The findings provide valuable insights into improving structural analysis and support more effective and efficient tree structural research and monitoring approaches.

Materials and methods
Study area
We focus on the tree architecture of two significant southern pine species, loblolly and longleaf pine. The loblolly pine dataset, consisting of 16 trees with heights ranging from 10.45 to 22.11 m, was collected at a site in the Millhopper Unit managed by the Forest Biology Research Cooperative (FBRC) at the University of Florida. This replicated experiment was established in 2010 to quantify stand-level dynamics of clonal stands[33]. The longleaf pine dataset includes 24 trees, with heights ranging from 7.47 to 26.88 m, collected from longleaf pine stands in Austin Cary Forest and naturally regenerated longleaf pine flatwoods in Myakka State Forest. Austin Cary Forest is managed by the School of Forest, Fisheries, and Geomatic Sciences at the University of Florida[34]. Myakka State Forest is situated within the Myakka River watershed, a region characterized by flatwoods, prairies, and wetlands[35] and is managed by the Florida Forest Service. All three sites are located in Florida, as shown in Fig. 1, with a subtropical and humid climate characterized by an average annual temperature of 24 °C and 1330 mm of precipitation[36].

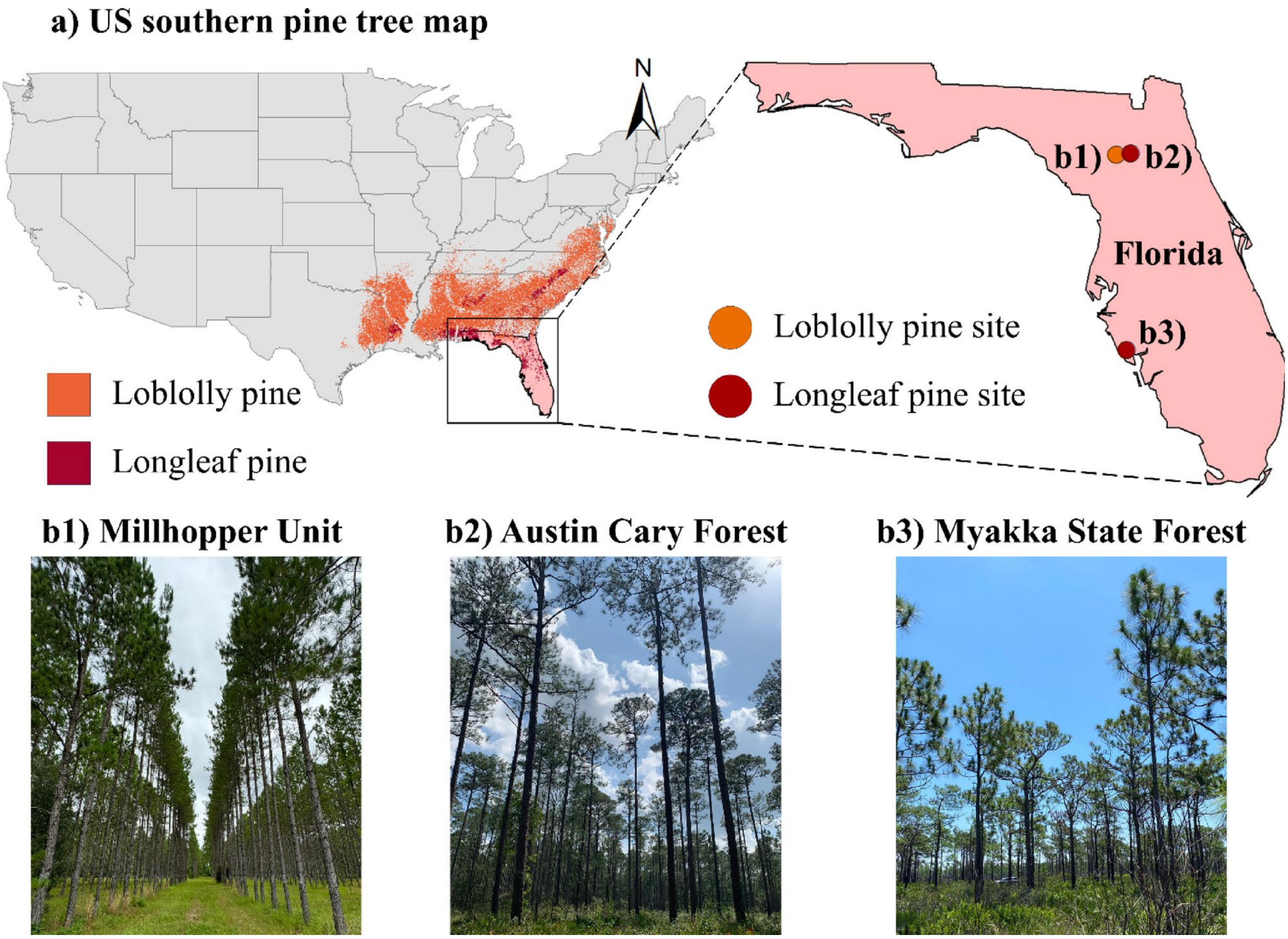

Fig. 1. Study area, plot locations, and plot characteristics at three sites in Florida. (**a**) Map of southern US pine tree distribution highlighting the state of Florida and the three study sites, generated using ArcGIS v10.8.2[37]. The distributions of longleaf and loblolly pine were visualized using tile layers[38,39] provided by the USDA Forest Service Forest Health Assessment and Applied Sciences Team (USFSForestHealth) through ArcGIS Online. (**b**) Overview of the three study sites: (**b1**) Millhopper Unit, (**b2**) Austin Cary Memorial Forest, and (**b3**) Myakka State Forest.

TLS data acquisition and pre-processing

Data collected included lidar point clouds acquired with RIEGL VZ 400i and GPS positioning with a differential GNSS RTK receiver[40] as shown in Fig. 2, on March 7, 2023 in the Austin Cary Memorial Forest; June 27, 2023 in the Myakka State Forest; and July 3, 2023 at the Millhopper Unit. We adopted a consistent scanning protocol across all sites, including standardized scanner settings, multiple scan angles per tree, and manual correction of motion artifacts, to enhance data comparability and reduce variability. Scans were conducted under calm and clear weather conditions to minimize environmental interference, but slight branch movements caused by residual wind could not be entirely avoided. A minimum of four TLS scans were taken for each tree to reduce occlusion. The angular resolution of 0.02 degrees in both azimuth and zenith, frequency 1,200 Hz, wavelength 1,550 nm, and beam divergence 0.35 mrad are the scan setup parameters that produced the initial point cloud density, approximately 100,000 points per tree. Each scan had a 360° horizontal field of view and a vertical field of view between −40° and 60°.

RiSCAN Pro 2.14.1[41] was used for point cloud registration and clipping. Noise in the raw data was removed using the Statistical Outlier Removal (SOR)[42] filter tool in CloudCompare[43] with the number of neighbors set to 10 and the standard deviation multiplier set to 3. In a few cases, duplicate branches were observed, likely resulting from wind-induced oscillations during scanning. These artifacts were manually removed to ensure structural accuracy. Recent reviews emphasize that careful acquisition protocols and post-processing—such as those employed here—can substantially mitigate these issues and support reliable volume modeling with QSMs[44–46]. Finally, the point cloud of individual trees was manually segmented into leaf and wood point clouds.

QSM algorithm selection

Before segmenting the tree point cloud using the leaf and wood segmentation methods, we first evaluated the performance of four different QSM algorithms based on manually segmented wood points. This preliminary evaluation established a baseline for comparison between the algorithms and helped identify which method

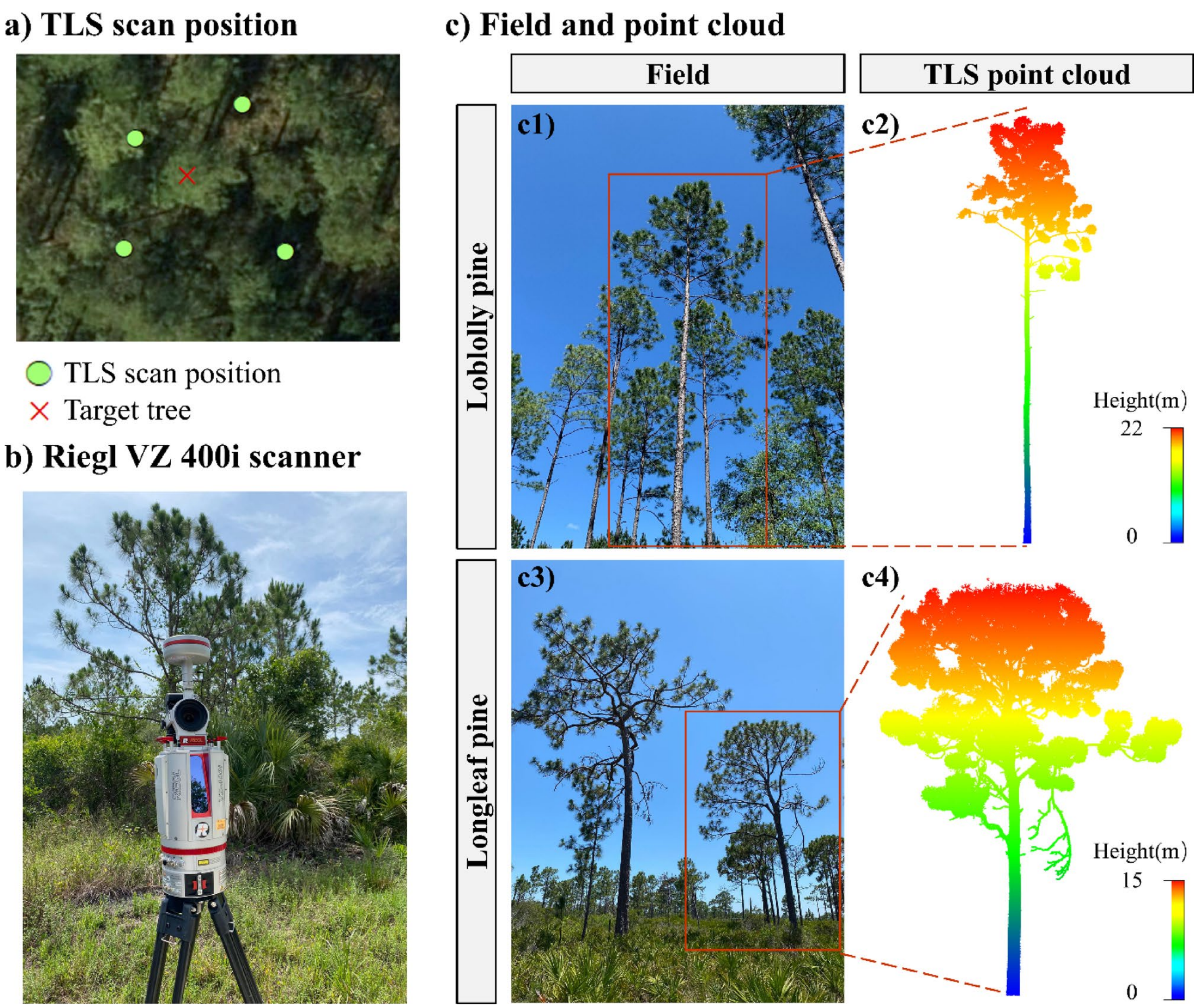

Fig. 2. Overview of TLS scanning setup and resulting point clouds for loblolly and longleaf pine trees. (**a**) TLS scanning design; (**b**) TLS system; (**c**) Trees in the field and their point clouds: (**c1-c2**) loblolly pine, (**c3-c4**): longleaf pine.

best aligned with our dataset and research objectives. We selected four QSM algorithms for this comparison: TreeQSM[18] AdQSM[13] aRchi[47] and SimpleForest[45] as shown in Supplementary Table S1. TreeQSM operates on a patch-based approach, while the other three methods first construct a skeleton before fitting the QSM.

TreeQSM[18] has been widely used to reconstruct QSMs[48–50] by dividing the point cloud into numerous patches. We used the *define_input* tool from TreeQSM version 2.4.1 to generate results by experimenting with different parameter combinations. Specifically, we estimated the trunk diameter near the base of the tree to define the initial parameters. *PatchDiam1* was set as approximately the trunk radius divided by 3, *PatchDiam2Min* as the trunk radius divided by 6, and *PatchDiam2Max* as the trunk radius divided by 2.5. These parameters were automatically adjusted based on tree height and point resolution. For this study, we defined *PatchDiam1*, *PatchDiam2Min*, and *PatchDiam2Max* as 2, 4, and 3, respectively, leading to 24 possible combinations for each tree. These parameter ratios were derived from previously published TreeQSM applications[49]. To avoid bias toward any specific configuration, we selected the result closest to the average volume across the 24 combinations as the final estimate for each tree. The entire procedure was executed in Matlab R2022a[51].

AdQSM[13] is based on the open-source AdTree[52] framework, which extracts the tree skeleton from the point cloud, simplifies it by merging closely spaced points, and reconstructs branches using least-squares cylindrical fitting and heteroscedasticity rules. We set different values for *Height_Segmentation* (HS) across multiple reconstructions (0.4, 0.5, 0.6, 0.7, 0.8, 0.9, 1.0) and averaged the results for each parameter to obtain the final volume metric. These parameter values follow guidance provided in the AdTree documentation and literature. Since the *Height_Segmentation* parameter determines vertical slicing for skeleton fitting, we visually evaluated reconstruction and selected the configuration with the most complete and realistic topology. The selected range offers flexibility for different crown shapes, but further optimization may be necessary for trees with more irregular branching habits. This process was implemented in Visual Studio 2017.

aRchi[47] is an R-based package that constructs a skeleton from a single tree point cloud, smooths the skeleton, and calculates the radius of each cylinder based on the distance from points to the skeleton. The layer thickness, representing the neighborhood search distance for points, was set to 0.1 m. We adjusted two key parameters for point cloud skeletonization: clustering distance for the entire point cloud (0.05, 0.1, and 0.15) and maximum search distance for skeleton building (0.2, 0.5, and 0.8). This resulted in 9 parameter combinations, and the final structural metrics were computed as the average of these results. The selected clustering and search distances were based on typical ranges used in previous aRchi studies and adjusted to suit the average point density of our TLS data. These parameters control both the granularity of skeleton nodes and the connectivity of branches. The entire process was implemented using R.

SimpleForest[45], an open-source plugin for the Computree platform, generates QSMs by first segmenting the point cloud into manageable cubic units to facilitate processing. It then simplifies the trunk and main branches by fitting cylindrical elements to create a skeletal representation. Using a hierarchical approach, SimpleForest progressively fits smaller branches by iterating through the connected components of the skeleton, ensuring a detailed and accurate reconstruction of the tree architecture. We used the new *VesselVolume* as proposed by Hackenberg and Bontemps (2023)[53] which is particularly effective in compensating for occlusion and noise in dense forest environments.

We selected the best-performing QSM algorithm based on the accuracy of the first-order branch number, which was compared to manually counted values. The first-order branch number, as illustrated in Fig. 3(f), serves as a critical structural metric for QSM evaluation because it is straightforward to quantify directly from the point cloud and provides a clear visual validation of reconstruction accuracy. This metric reflects the branching architecture of the tree and significantly influences estimates of branch volume, making it a reliable proxy for evaluating QSM performance. To analyze the agreement between the QSM-generated first-order branch numbers and the manually counted reference data, Bland-Altman plots were employed, visually illustrating the differences and biases.

Leaf and wood segmentation

Numerous studies have conducted detailed literature reviews on state-of-the-art leaf-wood separation algorithms[30] i.e. semantic segmentation. In this study, we selected four distinct open-source methods for comparison: TLSeparation, Graph-based, DBSCAN, and a deep learning-based method KPConv, as shown in Supplementary Figure S1. The first three methods are unsupervised, while the deep learning model is supervised. All of these methods utilize geometric metrics calculated from eigenvalues.

TLSeparation (TLSep)[54] integrates a Gaussian Mixture Model (GMM) with a path detection algorithm. Geometric features computed with varying neighborhood radii are fed into the GMM for point-by-point classification. After separation, four methods—mode smoothing, feature smoothing, clustering smoothing, and path smoothing—are used to further optimize the branch-leaf separation results. We used the generic_tree script from TLSep, setting the K-nearest neighbors (KNN) values for neighborhood search to [10, 210, 220, 150, 160]. The voxel size for both steps of the shortest path analysis was set to 0.13 m, and the retrace steps were set to 60, following the method outlined by Ali et al. (2024)[55].

The Density-Based Spatial Clustering of Applications with Noise (DBSCAN) method is a clustering algorithm that groups points based on their density. It relies on two key parameters: *eps* and *minimum cluster size*. The parameter *eps* defines the maximum distance between two points for them to be considered part of the same cluster, which we set to 0.03 m in this study. The *minimum cluster size* represents the smallest number of points required to form a cluster, set to 10 in this case. After clustering the points based on density, the linearity of each cluster is analyzed to classify it as either leaf or wood, considering the morphological characteristics of longleaf and loblolly pines.

The Graph-based method uses a KNN approach to segment the tree point cloud based on geometric features and point connectivity. First, a KNN graph is built by connecting each point to its nearest neighbors in spatial Euclidean space, using the 3D coordinates (X, Y, Z) of the points to determine distances. Geometric features, such as verticality and linearity, are then computed for each node. The graph is trimmed by removing edges where feature differences between connected points exceed the similarity threshold (0.15), ensuring that only points with similar characteristics remain linked. Clusters are then formed from the remaining connections, and the cluster-level geometric feature—linearity—is calculated to determine whether the cluster represents wood or leaf. Both Graph and DBSCAN are implemented using the R package lidUrb[56].

The deep learning method we employed is a variant of the Kernel Point Convolution (KPConv) network architecture[57]. KPConv is specifically designed for directly processing 3D point cloud data, utilizing kernel-based convolution operations to effectively capture geometric features and spatial relationships. We utilized KPConv Deformable, which allows kernel points to adapt their positions according to the local geometry of the point cloud. The grid size for the input data was set to 0.08 m. To mitigate the impact of large coordinates on model behavior, point coordinates were transformed to a local coordinate system. All implementations were based on the open-source framework Torch-Points3D[58] and tested on an NVIDIA Quadro RTX 5000 GPU. Our training dataset consisted of 27 randomly selected trees, including 10 loblolly pines and 17 longleaf pines. For data augmentation, we added random noise with sigma 0.01 and clip 0.05. Additionally, we applied random anisotropic scaling ranging from 0.9 to 1.1 and random rotations of 90, 180, and 270 degrees along the z-axis.

We applied four segmentation algorithms to extract the wood points and evaluated their performance using a manually segmented dataset as the reference. To generate the reference data, we manually annotated the point clouds in CloudCompare. The annotation process involved identifying and segmenting points into two categories: wood (trunks and branches) and leaf (foliage). Wood points were identified based on their structural characteristics, such as linear or cylindrical arrangements representing the trunk and primary branches. Leaf points were distinguished by their irregular and dispersed patterns, particularly reflecting the foliage structure

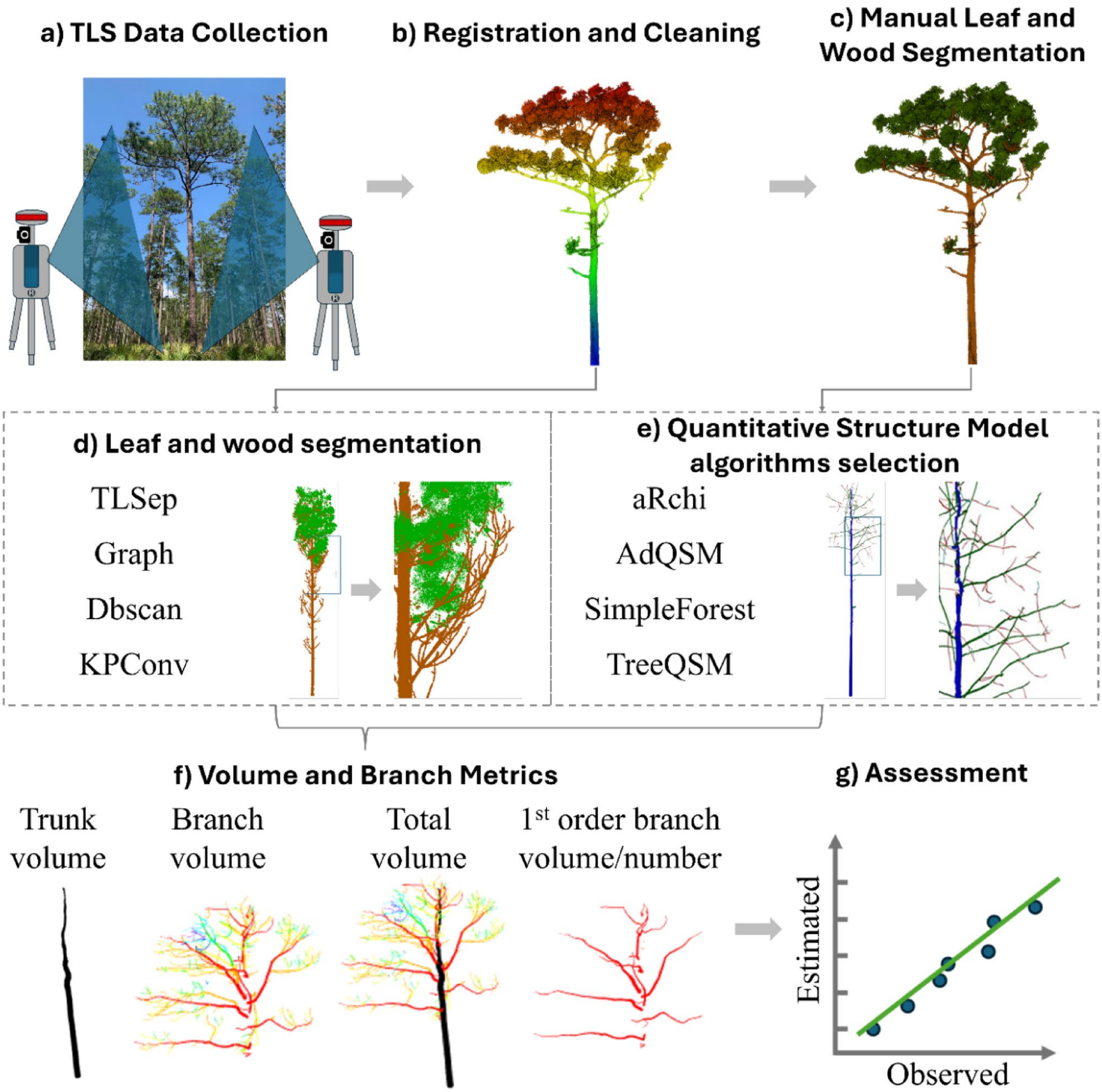

Fig. 3. Overview of the methodology. (**a**) TLS data collection. (**b**) Registration and cleaning. (**c**) Manual leaf and wood segmentation. (**d**) Leaf and wood segmentation. (**e**) Quantitative Structure Model algorithm selection. (**f**) Volume and branch metrics. (**g**) Assessment.

of longleaf pine and loblolly pine. Longleaf pine foliage typically consists of longer, more clustered needle groups, while loblolly pine foliage is characterized by shorter, denser needle arrangements. To ensure annotation accuracy, we iteratively refined the classification by visually inspecting the point clouds from multiple viewpoints. The final labeled point clouds served as the ground truth for evaluating the segmentation methods.

The performance was assessed through several key metrics. Overall accuracy (OA) measures the proportion of points that are correctly classified, offering a general indication of how well the segmentation method performs. Correctness evaluates the proportion of points predicted as wood that are actually wood, with higher correctness indicating fewer leaf points incorrectly classified as wood. This reduces noise in the QSM and ensures that the wood category is as accurate as possible. Completeness, on the other hand, measures the proportion of actual wood points that are correctly classified as wood. High completeness is essential for ensuring that most wood points are captured, avoiding under-segmentation. The F-score, calculated as the harmonic mean of correctness and completeness, provides a balanced assessment between the two, highlighting the algorithm's ability to minimize both false positives and false negatives. Finally, Incorrectness measures the proportion of leaf points misclassified as wood.

$$Overall\ accuracy = \frac{T_P + T_N}{T_P + T_N + F_P + F_N} \tag{1}$$

$$Correctness = \frac{T_P}{T_P + F_P} \tag{2}$$

$$Completeness = \frac{T_P}{T_P + F_N} \tag{3}$$

$$F\ score = 2 \times \frac{Completeness \times Correctness}{Completeness + Correctness} \tag{4}$$

$$Incorrectness = 1 - \frac{T_N}{T_N + F_N} \tag{5}$$

where: T_P is accurately segmented wood points, T_N is accurately segmented leaf points, F_P is inaccurately segmented wood points, and F_N is inaccurately segmented leaf points.

Finally, to evaluate the impact of segmentation methods on phenotype metrics, we used wood points segmented by the four approaches as input for the QSM algorithm determined. Metrics such as branch volume, trunk volume, and total volume were generated and compared to the reference metrics derived from manually segmented wood points. Branch volume represents the total cylindrical volume of all reconstructed branches in the tree. Trunk volume refers to the cylindrical volume of the main trunk. Total volume is the sum of branch and trunk volumes. To quantify the effect of different segmentation methods, we fitted a linear model to examine the relationship between the QSM-derived metrics using segmented wood points and those based on manually segmented wood points. The accuracy of the estimated metrics is evaluated with the coefficient of determination (R^2) of the linear model, root-mean-squared-difference (RMSD), and mean difference (MD), which would be computed as:

$$R^2 = \frac{\left[\sum_{i=1}^{n}\left(x_i - \bar{x}\right)\left(\widehat{x}_i - \bar{\widehat{x}}\right)\right]^2}{\sum_{i=1}^{n}\left(x_i - \bar{x}\right)^2 \sum_{i=1}^{n}\left(\widehat{x}_i - \bar{\widehat{x}}\right)^2} \tag{6}$$

$$RMSD = \sqrt{\frac{\sum_{i=1}^{n}\left(\widehat{x}_i - x_i\right)^2}{n}} \tag{7}$$

$$RMSD\% = \frac{RMSD}{\widehat{x}} \times 100\% \tag{8}$$

$$MD = \frac{\sum_{i=1}^{n}\left(\widehat{x}_i - x_i\right)}{n} \tag{9}$$

$$MD\% = \frac{MD}{\widehat{x}} \times 100\% \tag{10}$$

where: x_i represents the reference metric values (e.g., branch volume or number) generated from the QSM based on manually segmented wood points, $\widehat{x}_i$ represents the predicted metric values generated from the QSM using wood points segmented by one of the four leaf and wood segmentation methods, n is the total number of trees evaluated. The overview of this work is shown as Fig. 3.

Results

Comparative analysis of QSM methods

We used manually counted first-order branch numbers to evaluate and select the best-performing QSM algorithm, as shown in Fig. 4. For loblolly pine, AdQSM consistently underestimates branch numbers, particularly when the count is below 50. SimpleForest stays close to zero bias for most branch numbers, while aRchi increasingly overestimates branch numbers as they rise. TreeQSM remains near the zero-bias line, indicating strong agreement with reference data, making it the most reliable choice for loblolly pine. A similar trend is observed for longleaf pine, where TreeQSM and SimpleForest perform well. aRchi, however, consistently overestimates branch numbers, especially for larger counts. Based on these results, TreeQSM emerges as the most consistent and reliable algorithm for both species.

In addition to assessing accuracy, we performed an uncertainty analysis on TreeQSM-derived metrics by repeating the QSM generation 20 times from manually segmented wood points using the same parameter set. We recorded the resulting total volume, trunk, and branch volume for each repetition (see Supplementary Figure S2). The standard deviations were minimal for total and trunk volume across all trees and both species, indicating high consistency. Branch volume was also stable in longleaf pine, but two loblolly pine individuals showed noticeable variability, which may be attributed by occlusion or structural gaps in the upper crown.

Accuracy assessment of leaf and wood segmentation

Figure 5 presents the visual results of different leaf and wood segmentation methods. The manual reference, created by an experienced worker in CloudCompare, serves as the benchmark for comparison. The TLSep method shows reasonable performance but struggles with the misclassification of leaf points into the wood category, particularly in the upper crown regions. Both loblolly pine (a2) and longleaf pine (b2) exhibit some leaf points misclassified as wood points, with this issue being more pronounced in longleaf pine, indicating

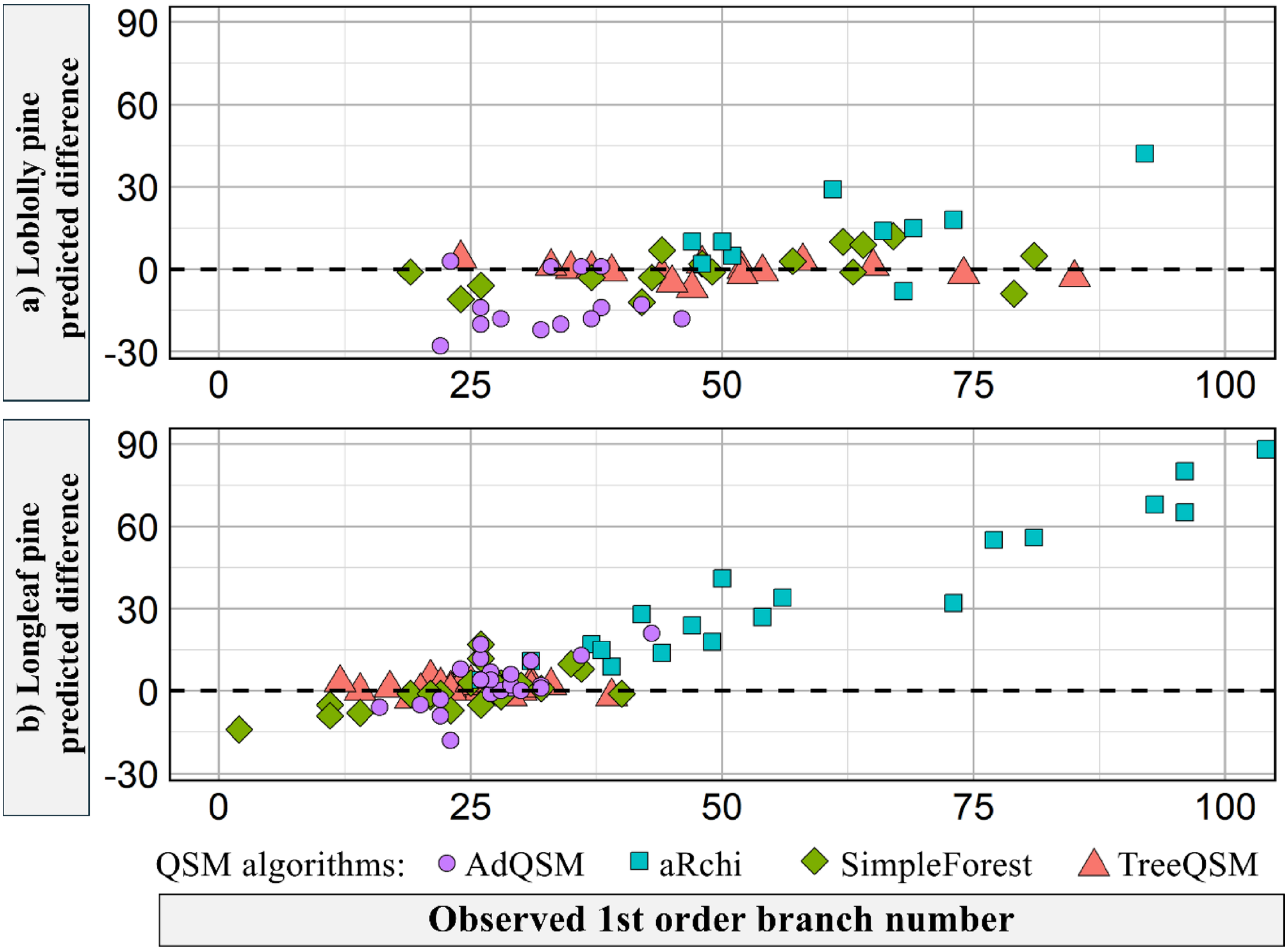

Fig. 4. Predicted difference in first-order branch number (n) between QSM-derived estimates and manual reference values for (**a**) loblolly pine and (**b**) longleaf pine. Each point represents one tree. Colors and shapes correspond to different QSM algorithms: purple circles = AdQSM, blue squares = aRchi, green diamonds = SimpleForest, and pink triangles = TreeQSM. The dashed line indicates zero difference.

challenges in accurately distinguishing dense leaf areas from wood. Graph (b3) improves on TLSep but still struggles with some misclassifications, particularly at the branch tips.

The DBSCAN method shows improved accuracy compared to TLSep and Graph. The results are closer to the manual reference, though small branches under the crown are misclassified as leaf points. The KPConv method delivers the most accurate segmentation, closely matching the manual reference. Both loblolly pine (a5) and longleaf pine (b5) exhibit minimal misclassification.

The quantitative assessment of wood and leaf segmentation is summarized in Table 1 and visually represented in the heatmap (Fig. 6). KPConv consistently outperforms the other methods across all metrics, achieving the highest Overall Accuracy (OA) for both loblolly pine (0.98) and longleaf pine (0.95), as well as the highest F score (0.98 for loblolly pine and 0.94 for longleaf pine). DBSCAN also performs well, particularly for loblolly pine, with an OA of 0.92 and an F score of 0.93.

Completeness, which measures the proportion of actual wood points correctly classified, shows that KPConv is the most effective at capturing the full structure of the tree. It achieves near-perfect scores of 0.97 for loblolly pine and 0.89 for longleaf pine. Graph also performs well, with high completeness for loblolly pine (0.98) and longleaf pine (0.91). However, TLSep struggles, particularly with loblolly pine (0.47), indicating it fails to capture important structural components like smaller branches and denser regions. Correctness, which measures how many of the points classified as wood are actually correct, highlights the strengths of KPConv and DBSCAN, both of which maintain very high correctness scores across both tree species. In contrast, TLSep performs poorly, with correctness scores of only 0.74 for loblolly pine and 0.68 for longleaf pine, reflecting frequent misclassification of leaf points as wood. Incorrectness is an important indicator of how much noise a segmentation method introduces. KPConv excels here with very low incorrectness, highlighting its precision. Graph also demonstrates low incorrectness for both species, while DBSCAN has slightly higher values (0.13 for loblolly pine and 0.12 for longleaf pine), indicating occasional misclassification. TLSep, again, underperforms with much higher incorrectness.

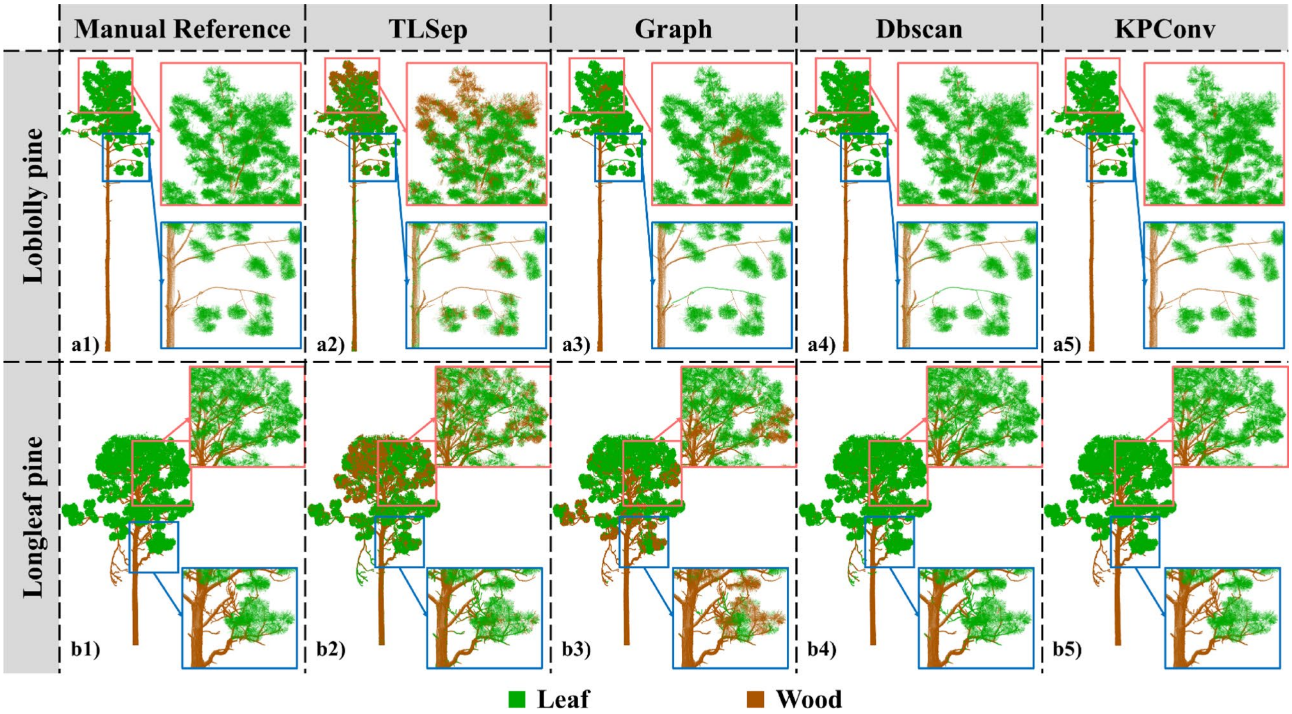

Fig. 5. Comparative visualization of leaf (green) and wood (brown) segmentation methods on point clouds of loblolly pine (**a1**-**a5**) and longleaf pine (**b1**-**b5**) using four different methods: TLSep, Graph, DBSCAN, and KPConv.

Species	Methods	Evaluation metrics				
		OA	F score	Correctness	Completeness	Incorrectness
Loblolly pine	TLSep	0.61	0.57	0.74	0.47	0.46
	Graph	0.86	0.89	0.81	0.98	0.03
	DBSCAN	0.92	0.93	0.99	0.87	0.13
	KPConv	0.98	0.98	0.99	0.97	0.04
Longleaf pine	TLSep	0.76	0.72	0.68	0.77	0.18
	Graph	0.80	0.79	0.69	0.91	0.08
	DBSCAN	0.90	0.87	0.94	0.81	0.12
	KPConv	0.95	0.94	0.99	0.89	0.07

Table 1. Summary of wood and leaf segmentation accuracy for loblolly and longleaf pine using four algorithms.

As shown in the heatmap Fig. 6, KPConv dominates, with the highest accuracy in both categories (96.2% for leaf and 99.5% for wood in loblolly pine). DBSCAN and Graph show less balanced performance. TLSep shows an overall weaker performance, especially in loblolly pine, where it correctly classifies only 54.1% of leaf. Canopy-level evaluation results are further summarized in Supplementary Table S2. KPConv consistently delivers high segmentation accuracy across all canopy layers, reflecting its robustness to structural variability and point density gradients. In contrast, TLSep exhibits pronounced declines in the lower canopy—most notably in loblolly pine. DBSCAN maintains competitive performance across canopy layers, especially in loblolly pine, while Graph shows reduced accuracy in middle layers.

Impact of segmentation accuracy on QSM-Derived volume metrics

Figure 7 compares the QSMs generated from wood points segmented by various algorithms, using the manual reference images (a1 and b1) as benchmarks for accurate tree structure. For both loblolly pine and longleaf pine, KPConv consistently generates the most accurate QSMs, closely matching the manual reference with minimal noise and well-replicated branch structures. In contrast, TLSep and Graph introduce significant noise and misclassifications, particularly in denser crown areas, where they struggle to distinguish finer branches. DBSCAN performs better than TLSep and Graph, offering cleaner results, but it still has difficulty accurately capturing finer branch details.

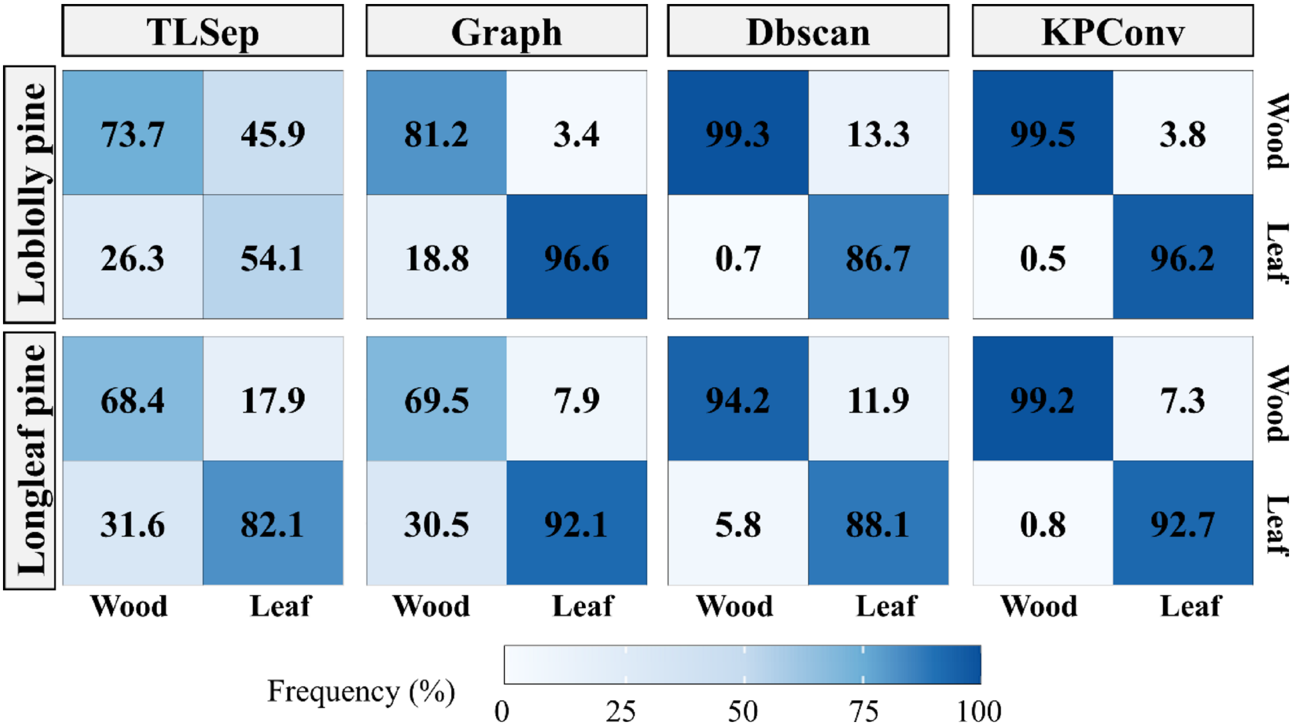

Fig. 6. Segmentation accuracy heatmap for wood and leaf points in loblolly and longleaf pine using four algorithms.

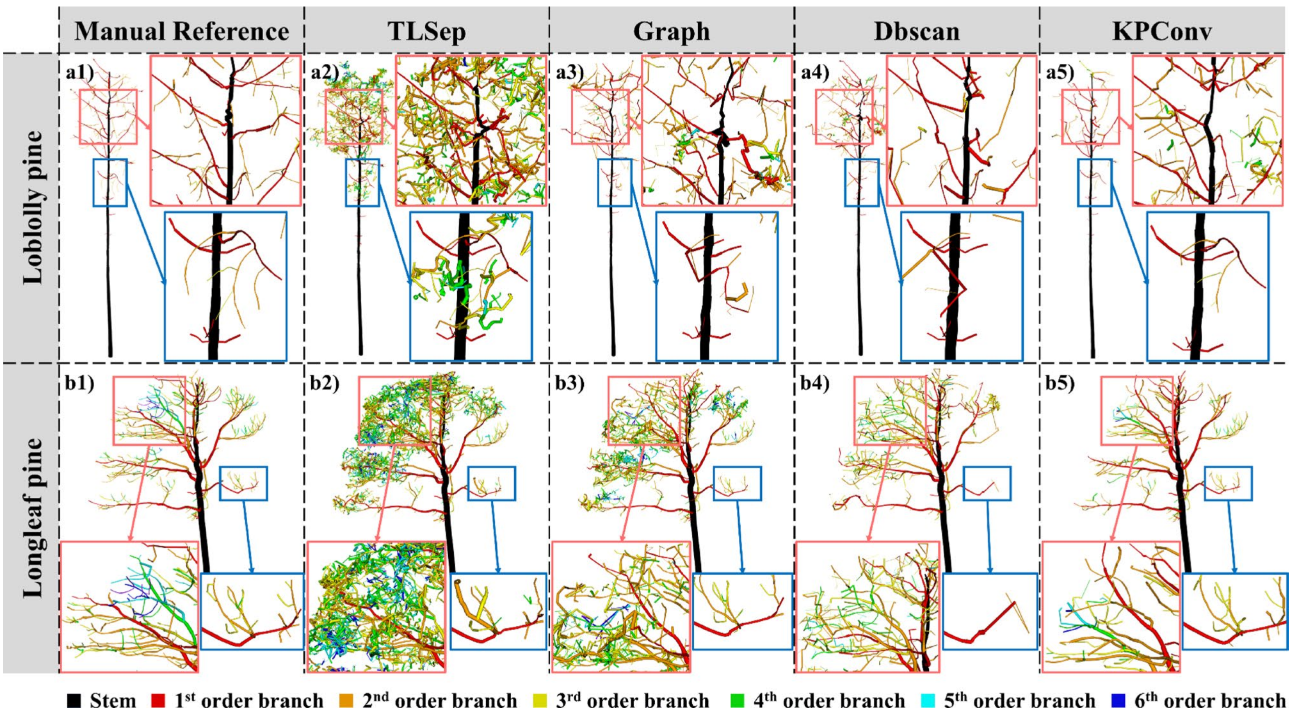

Fig. 7. Comparative visualization of QSMs generated from wood points segmented by four different methods (TLSep, Graph, DBSCAN, and KPConv) for loblolly pine (**a1**-**a5**) and longleaf pine (**b1**-**b5**).

Table 2 highlights that across both loblolly pine and longleaf pine, KPConv consistently delivers the highest accuracy, achieving near-perfect R^2 values for both trunk and total volume. DBSCAN also performs well, particularly in trunk and total volume estimates, though its performance slightly drops for branch volume in both species. TLSep shows lower accuracy overall, particularly for branch and total volume, while the Graph method underperforms especially for branch volume in loblolly pine.

The RMSD and MD values further confirm KPConv's superiority, with minimal deviations and biases in all volume categories for both species. DBSCAN also shows low RMSD and MD values, though its deviations increase slightly for branch volume, particularly in longleaf pine. In contrast, TLSep and Graph show much higher deviations, especially for branch volume.

For loblolly pine first order branch number, the Graph method (b) shows the highest accuracy in Fig. 8, with an R^2 of 0.94 and low RMSD and MD values, indicating a strong correlation between predicted and observed values. KPConv (d) and DBSCAN (c) also perform well, with KPConv showing slightly lower accuracy (R^2 = 0.83) and DBSCAN providing a solid balance between accuracy and consistency (R^2 = 0.85). TLSep (a) demonstrates moderate predictive accuracy with greater deviations, making it the least reliable in this group.

For longleaf pine first-order branch numbers, the performance trends shift slightly. DBSCAN (c) performs strongly, with an R^2 of 0.64, reflecting its ability to handle the complexity of branch structures in this species better than TLSep and Graph. KPConv (d) also continues to show strong performance, while Graph (b) shows a noticeable drop in accuracy compared to its performance in loblolly pine, indicating some variability depending on the species. TLSep again shows the lowest accuracy with the highest RMSD. For first-order branch volume, KPConv (d) excels with near-perfect R^2 values (0.98 for loblolly and 0.93 for longleaf) and minimal RMSD and MD, making it the most accurate method for volume prediction. DBSCAN (c) also performs very well, especially in loblolly pine, where it shows strong R^2 values and relatively low RMSD and MD, making it a reliable method for volume estimation. Graph (b), however, struggles with branch volume in loblolly pine (R^2 = 0.49), reflecting its inconsistency across different metrics. TLSep (a) also shows larger deviations and lower reliability in volume predictions.

Discussion

In this study, we offer a comprehensive evaluation of how leaf and wood segmentation methods and QSM algorithms jointly influence structural metrics estimation for two ecologically and economically significant southern pine species, loblolly and longleaf pine. By comparing four open-source leaf and wood algorithms (TLSeparation, Graph, DBSCAN, and KPConv) and QSM methods (TreeQSM, AdQSM, aRchi, and SimpleForest), we assess both traditional and deep learning-based approaches within a unified framework. This study highlights the critical role of segmentation accuracy in determining the reliability of QSM-derived metrics, such as branch and stem volume, which are fundamental for biomass estimation, carbon stock assessment, and forest management applications. By focusing on two evergreen species, this research also underscores the challenges posed by coniferous forest in high-density TLS data and the importance of integrating advanced segmentation and modeling approaches to reduce uncertainty in volume estimations.

Accuracy and efficiency of leaf and wood segmentation

This research focused on conifers, which exhibit more complex needle clusters compared to the leaves of broadleaf species commonly studied in previous segmentation research. In studies of broadleaf trees, segmentation accuracies have reached as high as 97.29%[59]. However, coniferous trees pose greater challenges due to their high needle density, non-planar needle orientation, and reduced spatial separation between leaf and wood points, which introduce occlusion and misclassification errors[60]. Reported segmentation accuracies for coniferous trees range from 0.68 to 0.95, averaging around 0.85[27,28,30–32]. For instance, Ma et al. (2015)[27] and Zhu et al. (2018)[32] examined Douglas fir and Spruce fir using rule-based or waveform-sensitive methods, with their segmentation

Species	Estimate accuracy		QSM-derived volumes											
			Trunk volume				Branch volume				Total volume			
			Methods											
			TLSep	Graph	DBSCAN	KPConv	TLSep	Graph	DBSCAN	KPConv	TLSep	Graph	DBSCAN	KPConv
Loblolly pine	R^2		0.93	1.00	0.99	1.00	0.60	0.14	0.71	0.86	0.72	0.94	0.98	1.00
	RMSD	Absolute (m^3)	0.05	0.01	0.02	0.01	0.30	0.09	0.03	0.01	0.31	0.09	0.04	0.01
		Relative (%)	16.00	2.89	6.16	3.56	679.95	211.71	63.41	19.73	83.70	25.77	12.31	1.84
	MD	Absolute (m3)	−0.00	−0.00	0.01	0.01	0.27	0.08	0.02	−0.00	0.26	0.08	0.02	0.00
		Relative (%)	−1.27	−0.53	2.61	1.95	604.72	184.53	33.80	−11.06	72.48	21.99	6.41	0.37
Longleaf pine	R^2		1.00	1.00	1.00	1.00	0.94	0.88	0.97	0.95	0.96	0.97	1.00	1.00
	RMSD	Absolute (m^3)	0.02	0.02	0.03	0.03	0.63	0.25	0.10	0.06	0.62	0.24	0.08	0.06
		Relative (%)	3.02	2.33	3.70	3.85	269.28	104.84	42.35	26.51	60.21	23.55	8.11	5.96
	MD	Absolute (m^3)	−0.01	−0.01	−0.01	−0.00	0.50	0.18	0.06	−0.03	0.49	0.17	0.06	−0.03
		Relative (%)	−1.36	−1.11	−0.77	−0.27	215.65	76.46	27.00	−13.41	48.09	16.56	5.56	−3.27

Table 2. Comparison of volume Estimation accuracy for loblolly and longleaf pine using QSMs generated from wood points segmented by four different algorithms.

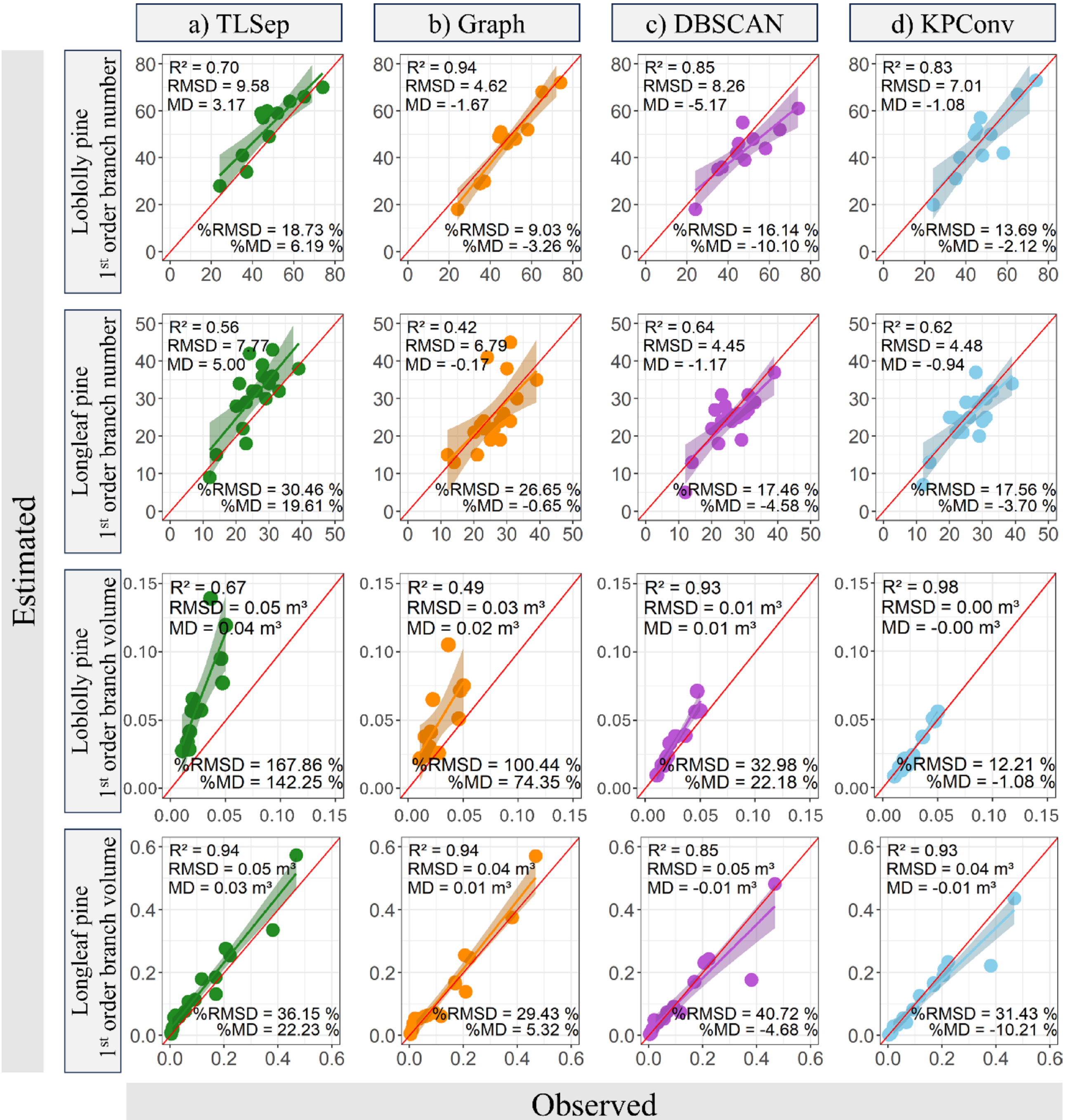

Fig. 8. Comparison of observed vs. estimated first-order branch number and branch volume for loblolly and longleaf pine using QSMs generated from TLS 3D point cloud segmented as wood components by four different algorithms (red line representing perfect agreement).

accuracy declined significantly in dense needle crowns. Xi et al. (2018)[31] proposed a 3D convolutional network for conifer stem filtering, while Wan et al. (2021)[30] developed a patch-wise separation approach that performed well in Darian larch plots. However, most of these studies were conducted on temperate conifers such as spruce, fir, or larch, which typically have shorter needles and more compact and symmetrical crowns. In contrast, the southern pines in our study—loblolly and longleaf—feature long, flexible needles clustered at the end of branches. These differences in foliage distribution and branch structure affect the point cloud characteristics, meaning that algorithms or parameterizations optimized for northern conifers may not generalize well to southern pine morphology. Moreover, the more irregular branching angles and less cylindrical branch shapes commonly seen in southern pines introduce a different set of considerations for QSM modeling that are distinct from those observed in boreal or temperate conifers.

In our study, we evaluated four segmentation algorithms and reported higher-than-average accuracies for coniferous trees: 0.92 (DBSCAN) and 0.98 (KPConv) for loblolly pine, and 0.90 and 0.95, respectively, for longleaf pine. These results demonstrate the applicability of both rule-based and learning-based approaches to morphologically distinct southern pine species, which to our knowledge have not been extensively studied in the context of leaf-wood segmentation. Beyond overall accuracy, we also assessed segmentation performance using correctness and completeness, following recent practices by Cai et al.[61] While DBSCAN showed higher incorrectness (0.13), it still achieved good completeness (0.87), capturing the majority of wood points. Graph, by contrast, exhibited excellent completeness (0.98 for loblolly pine) but lower correctness (0.81), suggesting an overclassification of leaf points as wood. These comparative metrics provide more nuanced insights into the relative strengths of each algorithm and their implications for downstream QSM accuracy, particularly in reconstructing finer branch volumes.

Efficiency is another critical factor in selecting segmentation methods. In terms of processing time, all four algorithms in our study handled point clouds with over six million points per tree. However, the time required to process these data varied significantly. Training the KPConv network on an NVIDIA Quadro RTX 5000 GPU took approximately 3 days. Once trained, inference time was approximately 2–5 min per tree, making it more competitive for large-scale applications. It also demonstrated robust performance across both loblolly and longleaf pine species, indicating its potential to generalize well without extensive retraining. For comparison, segmenting 40 trees took 10 h with the Graph-based method (~ 15 min/tree), 8 h with DBSCAN (~ 12 min/tree), and 2 days with TLSep (~ 72 min/tree). While KPConv outperforms in accuracy, it requires a substantial initial time investment for model training and the manual effort to create annotated training datasets. It also relies on high-performance GPUs, which may limit its accessibility for some field applications. This contrasts with methods like DBSCAN, which do not require training data and offer a favorable balance between computational efficiency and segmentation performance.

Considerations for model transferability

The structural characteristics of longleaf pine and loblolly pine significantly influence the accuracy of both 3D segmentation algorithms and QSM generation. Longleaf pine's open crown architecture, with long needles concentrated at the ends of branches in the upper crown and a largely branch-free trunk[62] reduces occlusion in point cloud data, simplifying leaf-wood separation. This branching facilitates accurate QSM generation, as fewer branches lead to clearer delineation of the stem and first-order branches. Conversely, loblolly pine's denser crown and more evenly distributed needles present greater challenges for segmentation, particularly in the mid-crown region where leaf and woody elements overlap, increasing the potential for misclassification, as seen in TLSep and Graph segmentation results.

Considering the structural uniqueness of different species, model transferability becomes a crucial challenge. Methods like DBSCAN and Graph rely on linearity-based clustering, which is species-specific and requires threshold adjustments to accurately define clusters. For example, Graph performed well with longleaf pine but required additional tuning for loblolly pine due to its more complex branching patterns. The need for species-specific thresholds adds to the complexity of applying these methods to diverse species[63]. In contrast, deep learning models like KPConv, despite requiring substantial manual annotation during training, generally demand less species-specific prior knowledge[19].

Our results underscore the importance of tailoring segmentation and QSM methods to match species-specific structural traits. To enhance model transferability, benchmarking these methods using public datasets that cover various species and environments is essential. Public datasets would allow standardized comparisons and help establish baseline performance metrics across different ecological contexts[64]. Although our study focuses on two southern pine species, the insights gained may be partially applicable to other coniferous species that share similar architectural features, such as slash pine or ponderosa pine. However, interspecies differences in crown density, needle arrangement, and branching patterns may introduce additional challenges for both segmentation and QSM modeling. To address these limitations, we encourage future research to evaluate algorithm performance across a broader spectrum of coniferous species. This would help clarify the boundaries of generalizability and support the development of more robust, adaptive, or species-agnostic segmentation frameworks suitable for large-scale forest applications.

Evaluation of QSM metrics

Integrating TLS with QSM has been widely recognized as an accurate approach for estimating direct tree parameters such as height, diameter at breast height (DBH), and trunk and branch volume[65–69]. In this study, we evaluated how different leaf and wood segmentation algorithms impact QSM-derived metrics. Among the tested methods, KPConv demonstrated the highest accuracy, achieving trunk and branch volume estimates with a near-perfect correlation to manually segmented wood points ($R^2 = 0.97$). These findings are consistent with Ali et al. (2024)[55] who reported that Random Forest achieved the highest overall accuracy and F-score, along with an excellent volume comparison ($R^2 = 0.98$).

While KPConv showed promising results in segmenting leaf and wood points and estimating volume metrics, the evaluation of accuracy in this study is based on comparisons with manually segmented data rather than ground truth derived from destructive harvesting. To our knowledge, destructively sampled QSM validation datasets for loblolly and longleaf pine at the individual branch level are currently lacking, which highlights a gap in the literature and the need for further empirical studies. Nevertheless, we ensured internal consistency by comparing multiple QSM algorithms and evaluating correlations with manually segmented reference datasets. In the broader context, other studies have validated QSM-derived metrics with harvested data in different species. For example, Calders et al. (2022)[70] demonstrated the utility of TLS and QSM in achieving accurate volume measurements with destructively harvested trees, while Martin-Ducup et al. (2021)[71] showed median relative errors ranging from 39 to 115% in fully automated QSM pipelines.

To ensure robust and stable results in generating QSMs, we tested four QSM models and ultimately selected the most suitable approach for our dataset. TreeQSM emerged as the optimal algorithm for modeling southern pine trees, particularly based on first-order branch number metrics. However, it is important to acknowledge the limitations of TreeQSM versions, as highlighted by Morales and MacFarlane (2024)[49]. The latest version, 2.4.x, further enhanced higher-order branch reconstruction and tree topology but applied a more relaxed taper constraint, leading to overestimation of branch volume. In our study, we used TreeQSM v2.4.1, which may not provide the most accurate estimates for absolute volume due to its overestimation of higher-order branch volume. However, as our analysis focuses on the relative accuracy of different leaf and wood segmentation algorithms rather than comparisons with ground truth, v2.4.1 proved suitable for evaluating the relative performance of these methods. To assess reconstruction consistency, we performed 20 repeated QSM reconstructions using the same parameter set for each segmentation output. The resulting coefficients of variation for trunk, branch, and total volume were generally low across all methods, indicating that TreeQSM v2.4.1 is robust under fixed settings. It also highlights that segmentation accuracy affects reconstruction stability—methods with more accurate wood point separation, such as KPConv, consistently yielded lower uncertainty (see Supplementary Figure S3).

As noted in previous studies, TLS-QSM workflows face challenges in reconstructing fine branch structures, particularly for branches below 3 cm in diameter[72]. To address current limitations, we are further leveraging the detailed structural data collected during destructive harvesting, including first-order branch angle, basal diameter, and length. These traits will be used to evaluate the topological fidelity of QSMs and to identify systematic deviations across models. Building on this dataset, we aim to develop phenotype-based error diagnostics and model correction strategies—for example, by applying regression analysis to relate QSM-derived and field-measured traits, or using these measurements as priors to constrain reconstruction algorithms. In addition to trait-based correction, deep learning-based point cloud completion methods such as PoinTr[73] may help recover missing fine-scale structures in sparsely sampled or occluded regions, offering a complementary approach to structural refinement. It's also necessary to evaluate the potential of next-generation QSM tools, such as TreeGraph[69] which allow probabilistic fitting of uncertain structures and may better accommodate variability in conifer crown morphology. These directions will provide a more comprehensive evaluation framework for QSM reliability at the fine-branch level and support the development of more adaptive and biologically consistent modeling pipelines.

Conclusion

The rapid advancements in TLS point cloud data processing have enabled forest researchers to obtain detailed, fine-scale information about trees. Our study provides a comprehensive framework for evaluating the accuracy and effectiveness of various segmentation methods (TLSep, Graph, DBSCAN, and KPConv) in generating reliable QSMs for southern pine trees. From our findings, several key conclusions can be drawn. First, KPConv consistently emerged as the most accurate method for segmenting wood and leaf points, leading to highly reliable QSMs across trunk, branch, and total volume estimates. Although DBSCAN showed slightly lower accuracy, it offers a valuable balance between computational efficiency and accuracy, making it a practical option in scenarios where resources or time are constrained. Second, our study highlights the critical impact of segmentation accuracy on the reliability of QSM-derived metrics, emphasizing the need for careful selection of segmentation methods based on specific research or management goals. This is particularly relevant for forest managers seeking to implement TLS in forest monitoring and management. Finally, despite the success of these methods, challenges remain in fully capturing fine branch details, especially in dense canopy regions. Future research should focus on refining these segmentation techniques and validating their performance through additional fieldwork. The insights gained from this study contribute to the ongoing development of non-destructive and efficient tools for forest structural research, offering a promising direction for expanding the use of TLS across diverse forest ecosystems.

Data availability

The datasets used in this study may be available from the corresponding author upon reasonable request. Due to data and genotype ownership and institutional agreements, access may be subject to approval and require a signed data use agreement. Researchers interested in accessing the data are encouraged to contact the corresponding author with a brief description of the intended use. The authors declare that they have no known competing financial interests or personal relationships that could have appeared to influence the work reported in this paper.

Received: 15 January 2025; Accepted: 30 June 2025
Published online: 08 July 2025

References

1. Jokela, E. J., Martin, T. A. & Vogel, J. G. Twenty-Five years of intensive forest management with Southern pines: important lessons learned. *J. Forest.* **108**, 338–347 (2010).
2. Shephard, N. T., Narine, L., Peng, Y. & Maggard, A. Climate smart forestry in the Southern united States. *Forests* **13**, 1460 (2022).
3. Guo, J., Prestemon, J. & Johnston, C. Forest market outlook in the Southern united States. *For. Policy Econ.* **157**, 103091 (2023).
4. Coyle, D. R. et al. A review of Southern pine decline in North America. *For. Ecol. Manag.* **349**, 134–148 (2015).

5. Van Lear, D. H. & Harlow, R. F. Fire in the eastern United States: influence on wildlife habitat. in *The Role of Fire in Nongame Wildlife Management and Community Restoration: Traditional Uses and New Directions, Proc. Special Workshop, Nashville, TN. Gen. Tech. Rep. NE-288* 2–10 (2000).
6. Wear, D. N. & Greis, J. G. Southern forest resource assessment: summary of findings. *J. Forest.* **100**, 6–14 (2002).
7. Pretzsch, H. Forest dynamics, growth, and yield: A review, analysis of the present state, and perspective. in *Forest Dynamics, Growth and Yield: From Measurement to Model* 1–39 (Springer, 2008).
8. Liang, X. et al. Terrestrial laser scanning in forest inventories. *ISPRS J. Photogrammetry Remote Sens.* **115**, 63–77 (2016).
9. Bienert, A., Georgi, L., Kunz, M., Maas, H. G. & Von Oheimb, G. Comparison and combination of mobile and terrestrial laser scanning for natural forest inventories. *Forests* **9**, 395 (2018).
10. Xia, S. et al. Detecting stems in dense and homogeneous forest using Single-Scan TLS. *Forests* **6**, 3923–3945 (2015).
11. Momo Takoudjou, S. et al. Using terrestrial laser scanning data to estimate large tropical trees biomass and calibrate allometric models: A comparison with traditional destructive approach. *Methods Ecol. Evol.* **9**, 905–916 (2018).
12. Calders, K. et al. Nondestructive estimates of above-ground biomass using terrestrial laser scanning. *Methods Ecol. Evol.* **6**, 198–208 (2015).
13. Fan, G. et al. A new quantitative approach to tree attributes Estimation based on lidar point clouds. *Remote Sens.* **12**, 1779 (2020).
14. Hu, M. et al. A new method to estimate branch biomass from terrestrial laser scanning data by bridging tree structure models. *Ann. Botany*. **128**, 737–752 (2021).
15. Hui, Z. et al. A Self-Adaptive optimization individual tree modeling method for terrestrial lidar point clouds. *Remote Sens.* **14**, 2545 (2022).
16. Disney, M. I. et al. Weighing trees with lasers: advances, challenges and opportunities. *Interface Focus*. **8**, 20170048 (2018).
17. Wang, D. et al. LeWoS: A universal leaf-wood classification method to facilitate the 3D modelling of large tropical trees using terrestrial lidar. *Methods Ecol. Evol.* **11**, 376–389 (2020).
18. Raumonen, P. et al. Fast automatic precision tree models from terrestrial laser scanner data. *Remote Sens.* **5**, 491–520 (2013).
19. Han, T. & Sánchez-Azofeifa, G. A. A deep learning time series approach for leaf and wood classification from terrestrial lidar point clouds. *Remote Sens.* **14**, 3157 (2022).
20. Béland, M., Baldocchi, D. D., Widlowski, J. L., Fournier, R. A. & Verstraete, M. M. On seeing the wood from the leaves and the role of voxel size in determining leaf area distribution of forests with terrestrial lidar. *Agric. For. Meteorol.* **184**, 82–97 (2014).
21. Tan, K., Zhang, W., Dong, Z., Cheng, X. & Cheng, X. Leaf and wood separation for individual trees using the intensity and density data of terrestrial laser scanners. *IEEE Trans. Geosci. Remote Sens.* **59**, 7038–7050 (2021).
22. Calders, K. et al. Evaluation of the range accuracy and the radiometric calibration of multiple terrestrial laser scanning instruments for data interoperability. *IEEE Trans. Geosci. Remote Sens.* **55**, 2716–2724 (2017).
23. Wang, D., Hollaus, M. & Pfeifer, N. Feasibility of machine learning methods for separating wood and leaf points from terrestrial laser scanning data. *ISPRS Annals Photogrammetry Remote Sens. & Spat. Inform. Sciences* **4**, 157–164 (2017).
24. Krishna Moorthy, S. M., Calders, K., Vicari, M. B. & Verbeeck, H. Improved supervised Learning-Based approach for leaf and wood classification from lidar point clouds of forests. *IEEE Trans. Geosci. Remote Sens.* **58**, 3057–3070 (2020).
25. Chen, S. et al. The impact of leaf-wood separation algorithms on aboveground biomass Estimation from terrestrial laser scanning. *Remote Sens. Environ.* **318**, 114581 (2025).
26. Henrich, J. & van Delden, J. Towards general deep-learning-based tree instance segmentation models. Preprint at https://arxiv.org/abs/2405.02061 (2024).
27. Ma, L. et al. Improved salient feature-based approach for automatically separating photosynthetic and nonphotosynthetic components within terrestrial lidar point cloud data of forest canopies. *IEEE Trans. Geosci. Remote Sens.* **54**, 679–696 (2015).
28. Shcherbcheva, A. et al. *Int. Archives Photogrammetry*, Remote Sensing and Spatial Information Sciences **XLVIII–1–W2–2023**, 1787–1794 (2023).
29. Tian, Z. & Li, S. Graph-Based Leaf–Wood separation method for individual trees using terrestrial lidar point clouds. *IEEE Trans. Geosci. Remote Sens.* **60**, 1–11 (2022).
30. Wan, P. et al. A novel and efficient method for wood–leaf separation from terrestrial laser scanning point clouds at the forest plot level. *Methods Ecol. Evol.* **12**, 2473–2486 (2021).
31. Xi, Z., Hopkinson, C. & Chasmer, L. Filtering stems and branches from terrestrial laser scanning point clouds using deep 3-D fully convolutional networks. *Remote Sens.* **10**, 1215 (2018).
32. Zhu, X. et al. Foliar and Woody materials discriminated using terrestrial lidar in a mixed natural forest. *Int. J. Appl. Earth Obs. Geoinf.* **64**, 43–50 (2018).
33. Ramalho de Oliveira, L. F. et al. Moving to automated tree inventory: comparison of UAS-Derived lidar and photogrammetric data with manual ground estimates. *Remote Sens.* **13**, 72 (2021).
34. Fox, T. R., Jokela, E. J. & Allen, H. L. The development of pine plantation silviculture in the Southern united States. *J. Forest.* **105**, 337–347 (2007).
35. Hutchens, L. et al. Projecting the long-term effects of large-scale human influence on the Spatial and functional persistence of extant longleaf pine ecosystems in the Florida Flatwoods pyrome. *Conserv. Sci. Pract.* **6**, e13187 (2024).
36. Haque, S. E. The effects of climate variability on florida's major water resources. *Sustainability* **15**, 11364 (2023).
37. Esri. *ArcGIS Desktop, version 10.8.2*. https://www.esri.com/en-us/arcgis/products/arcgis-desktop/overview (2020).
38. USFS Forest Health. *Longleaf Pine*. https://www.arcgis.com/home/item.html?id=51487841c8e24e21a563ede96326ac38 (2019).
39. USFS Forest Health. *Loblolly Pine*. https://www.arcgis.com/home/item.html?id=3bc8457e61cb4a959f58ac1bda41750e (2019).
40. Klauberg, C. et al. Post-Hurricane damage severity classification at the individual tree level using terrestrial laser scanning and deep learning. *Remote Sens.* **15**, 1165 (2023).
41. RIEGL Laser Measurement Systems GmbH. *RiSCAN PRO*, *version 2.14.1* (Horn, Austria, 2022).
42. Rusu, R. B., Blodow, N., Marton, Z., Soos, A. & Beetz, M. Towards 3D object maps for autonomous household robots. In *Proceedings of the 2007 IEEE/RSJ International Conference on Intelligent Robots and Systems (IROS)* 3191–3198 (IEEE, 2007).
43. CloudCompare. *CloudCompare, version 2.12* [GPL software] (2022).
44. Demol, M. et al. Estimating forest above-ground biomass with terrestrial laser scanning: current status and future directions. *Methods Ecol. Evol.* **13**, 1628–1639 (2022).
45. Hackenberg, J., Spiecker, H., Calders, K., Disney, M. & Raumonen, P. SimpleTree—an efficient open source tool to build tree models from TLS clouds. *Forests* **6**, 4245–4294 (2015).
46. Wilkes, P. et al. Terrestrial laser scanning to reconstruct branch architecture from harvested branches. *Methods Ecol. Evol.* **12**, 2487–2500 (2021).
47. Martin-Ducup, O. & Lecigne, B. *aRchi: Quantitative structural model ('QSM') treatment for tree architecture.* R package version 2.0.0 (2022). https://github.com/umr-amap/aRchi
48. Dalla Corte, A. P. et al. Applying High-Resolution UAV-LiDAR and quantitative structure modelling for estimating tree attributes in a Crop-Livestock-Forest system. *Land* **11**, 507 (2022).
49. Morales, A. & MacFarlane, D. W. Reducing tree volume overestimation in quantitative structure models using modeled branch topology and direct twig measurements. *Forestry* **98**, 394–409 (2025).
50. Winberg, O. et al. Branch information extraction from Norway Spruce using handheld laser scanning point clouds in nordic forests. *ISPRS Open. J. Photogrammetry Remote Sens.* **9**, 100040 (2023).
51. MathWorks, Inc. *MATLAB and Statistics Toolbox, Release 2022a* (Natick, Massachusetts, 2022).

52. Du, S., Lindenbergh, R., Ledoux, H., Stoter, J. & Nan, L. AdTree: accurate, detailed, and automatic modelling of Laser-Scanned trees. *Remote Sens.* **11**, 2074 (2019).
53. Hackenberg, J. & Bontemps, J. D. Improving quantitative structure models with filters based on allometric scaling theory. *Applied Geomatics* **15**, 1019–1029 (2023).
54. Vicari, M. B. et al. Leaf and wood classification framework for terrestrial lidar point clouds. *Methods Ecol. Evol.* **10**, 680–694 (2019).
55. Ali, M., Lohani, B., Hollaus, M. & Pfeifer, N. Benchmarking Geometry-Based Leaf-Filtering algorithms for tree volume Estimation using terrestrial lidar scanners. *Remote Sens.* **16**, 1021 (2024).
56. Lecigne, B. *lidUrb: Urban trees analyses from terrestrial laser scanning*. R package version 1.0 (2023). https://github.com/Blecigne/lidUrb
57. Thomas, H. et al. KPConv: Flexible and deformable convolution for point clouds. *Preprint at* https://arxiv.org/abs/1904.08889 (2019).
58. Chaton, T., Chaulet, N., Horache, S., Landrieu, L. & Torch-Points, D. A modular multi-task framework for reproducible deep learning on 3D point clouds. *In International Conference on 3D Vision (3DV)* 1–10 (IEEE, 2020).
59. Jiang, T. et al. LWSNet: A Point-Based segmentation network for Leaf-Wood separation of individual trees. *Forests* **14**, 1303 (2023).
60. Åkerblom, M. et al. Non-intersecting leaf insertion algorithm for tree structure models. *Interface Focus.* **8**, 20170045 (2018).
61. Cai, S., Zhang, W., Zhang, S., Yu, S. & Liang, X. Branch architecture quantification of large-scale coniferous forest plots using UAV-LiDAR data. *Remote Sens. Environ.* **306**, 114121 (2024).
62. Brockway, D. G., Outcalt, K. W. & Boyer, W. D. Longleaf pine regeneration ecology and methods. in *The Longleaf Pine Ecosystem: Ecology, Silviculture, and Restoration* (eds. Jose, S., Jokela, E. J. & Miller, D. L.) 95–133 (Springer, New York, 2006).
63. Ferrara, R. et al. An automated approach for wood-leaf separation from terrestrial LIDAR point clouds using the density based clustering algorithm DBSCAN. *Agric. For. Meteorol.* **262**, 434–444 (2018).
64. Puliti, S. et al. Benchmarking tree species classification from proximally-sensed laser scanning data: introducing the FOR-species20K dataset. *Preprint at* https://arxiv.org/abs/2408.06507 (2024).
65. Arseniou, G., MacFarlane, D. W., Calders, K. & Baker, M. Accuracy differences in aboveground Woody biomass Estimation with terrestrial laser scanning for trees in urban and rural forests and different leaf conditions. *Trees* **37**, 761–779 (2023).
66. Demol, M., Calders, K., Verbeeck, H. & Gielen, B. Forest above-ground volume assessments with terrestrial laser scanning: a ground-truth validation experiment in temperate, managed forests. *Ann. Botany*. **128**, 805–819 (2021).
67. Kükenbrink, D. et al. Above-ground biomass references for urban trees from terrestrial laser scanning data. *Ann. Botany* **128**, 709–724 (2021).
68. Xi, Z., Chasmer, L. & Hopkinson, C. Delineating and reconstructing 3D forest fuel components and volumes with terrestrial laser scanning. *Remote Sens.* **15**, 4778 (2023).
69. Yang, W. et al. Treegraph: tree architecture from terrestrial laser scanning point clouds. *Remote Sens. Ecol. Conserv.* **10**, 755–774 (2024).
70. Calders, K. et al. Laser scanning reveals potential underestimation of biomass carbon in temperate forest. *Ecol. Solutions Evid.* **3**, e12197 (2022).
71. Martin-Ducup, O. et al. Evaluation of automated pipelines for tree and plot metric Estimation from TLS data in tropical forest areas. *Ann. Botany*. **128**, 753–766 (2021).
72. Morhart, C. et al. Limitations of estimating branch volume from terrestrial laser scanning. *Eur. J. For. Res.* **143**, 687–702 (2024).
73. Yu, X. et al. Pointr: Diverse point cloud completion with geometry-aware transformers. in *Proceedings of the IEEE/CVF international conference on computer vision* 12498–12507 (2021).

Acknowledgements
This research was funded by the Forest Biology Research Cooperative (FBRC) and Cooperative Forest Genetics Research Program (CFGRP) at the School of Forest, Fisheries, and Geomatics Sciences (SFFGS) at the University of Florida (UF); supported by the intramural research program of the U.S. Department of Agriculture, National Institute of Food and Agriculture, through the Rapid Response to Extreme Weather Events Across Food and Agricultural Systems initiative (Grant #2023-68016-39039); the Strategic Environmental Research and Development Program (SERDP) project RC20-1346; and NASA's ICESat-2 program (Grant #80NSSC23K0941), Carbon Monitoring System (CMS, Grant #80NSSC23K1257), and Commercial Smallsat Data Scientific Analysis (CSDSA, Grant #80NSSC24K0055).

Author contributions
J. X. and C. A. S.: conceptualization, methodology, data collection, data processing, and writing up. T. A. M. and G. F. P.: funding acquisition, project administration, conceptualization, writing – review & editing. K. B., M. G. A., and C. K.: contributed to data collection and data processing. J. W. A., M. A. G., K. C., I. B., (A) P. D. C., C. H., M. (B) S., A. T. H.: contributed to the interpretation, quality control, and revisions of the manuscript.

Declarations

Competing interests
The authors declare that they have no known competing financial interests or personal relationships that could have appeared to influence the work reported in this paper.

Additional information
Supplementary Information The online version contains supplementary material available at https://doi.org/10.1038/s41598-025-09681-w.

Correspondence and requests for materials should be addressed to J.X. or C.A.S.

Reprints and permissions information is available at www.nature.com/reprints.

Publisher's note Springer Nature remains neutral with regard to jurisdictional claims in published maps and institutional affiliations.